Complex permittivity measurement using metamaterial split ring resonators

Sreedevi P. Chakyar, Sikha K. Simon, C. Bindu, Jolly Andrews, and V. P. Joseph

Citation: Journal of Applied Physics **121**, 054101 (2017); doi: 10.1063/1.4975111
View online: http://dx.doi.org/10.1063/1.4975111
View Table of Contents: http://aip.scitation.org/toc/jap/121/5
Published by the American Institute of Physics

Complex permittivity measurement using metamaterial split ring resonators

Sreedevi P. Chakyar, Sikha K. Simon, C. Bindu, Jolly Andrews, and V. P. Joseph
Department of Physics, Christ College (Autonomous), Irinjalakuda, University of Calicut, Kerala, India

(Received 4 October 2016; accepted 16 January 2017; published online 1 February 2017)

A direct and efficient method for determining the complex permittivity of materials at microwave frequencies using a Split Ring Resonator (SRR) metamaterial structure is presented. A single SRR unit fabricated on a substrate arranged between transmitting and receiving probes acts as a test probe. Dielectric samples having at least one flat surface of area greater than or equal to the area of SRR structure are used as test samples. The relative permittivity and the loss tangent of the dielectric are evaluated from the resonant frequency shift and the bandwidth of the SRR resonator, by placing the sample over it. The *LC* resonance of the SRR test probe is theoretically related to the permittivity by considering its equivalent circuit in terms of the dielectric filled capacitances formed on the upper and lower surfaces of the SRR. The permittivity measurements are performed using test probes of different resonant frequencies, and the results are compared with the values obtained by the cavity perturbation method. *Published by AIP Publishing*.
[http://dx.doi.org/10.1063/1.4975111]

I. INTRODUCTION

A precise determination of the dielectric constant of materials having different sizes and shapes is very important in the characterisation studies and in its industrial, scientific, and medical applications pertaining to the microwave region. The knowledge of dielectric parameters helps us to identify and study the interaction of electromagnetic waves with materials which is essential for the development of manifold instrumentation and sensor applications in fields such as biomedical and food.[1] Various methods are proposed in the literature for dielectric studies in the microwave/RF region. Some of the commonly used techniques include free space methods, transmission/reflection methods, resonant methods, and near-field sensor methods.[2–4]

Out of the many methods used for the permittivity measurement, the resonant method is often preferred due to its high precision and sensitivity. Two major kinds of resonant methods are resonator method and resonant perturbation method. In the former, the sample itself acts as a resonator, and in the latter, the sample changes the resonant properties of the resonator. We are introducing a resonant perturbation method for the measurement of the complex permittivity of low loss and low dielectric value materials using metamaterial Split Ring Resonators (SRRs). SRRs are constituent molecules of metamaterials showing a negative permeability.[5–7] The procedure for determination of the effective negative permeability and permittivity of metamaterial SRRs is reported.[8,9] Tunability of the resonant frequency of SRR with the changes in environmental parameters makes it possible to use them in the dielectrometric studies of solids and liquids.[10–14] Accordingly, SRRs find applications in the field of sensors, magneto-inductive devices, and material characterisation.[15–20] The effect of the dielectric environment on the resonant frequency of SRR is well studied.[21–25] But the determination of permittivity of a dielectric material based on the shift in the resonant frequency of metamaterial molecules is seldom found in the literature. By using transmission line based Complementary Split Ring Resonators (CSRR), Boybay and Ramahi[26] have proposed a method for measuring the real part of the permittivity of very low loss dielectric samples. It is based on an extraction technique where some samples with known values of the dielectric constant are a pre-requisite. Another transmission line based extraction procedure proposed by Galindo-Romera *et al.*[27] describes the permittivity characterization of solid and liquid materials using SRRs. They have employed empirical relations for the analysis of the complex permittivity.

In this paper, by working on the resonant perturbation method, using a single SRR as a movable test probe, we introduce a direct and easy technique to precisely determine both the real and imaginary parts of the permittivity of different solid materials. A detailed theoretical analysis based on the characteristic parameters of the SRR, along with its experimental confirmation using different test probes resonating at different frequencies, is presented. The results are verified using a standard cavity perturbation technique.

II. THEORETICAL MODEL

A negative permeability metamaterial molecule SRR, usually fabricated on a planar dielectric substrate, composes of two concentric metal rings of width c and spacing d. The radius of the inner ring is r. The two metal rings have small splits on the diametrically opposite sides of the structure. Schematic representation of the SRR structure is shown in Fig. 1.

SRR shows an *LC* resonant nature, which arises from the capacitance and the inductance of the two rings due to charges and currents induced in them by the magnetic component of the applied electromagnetic field. The resonant frequency of the SRR is given by

$$f = \frac{1}{2\pi\sqrt{LC}}, \tag{1}$$

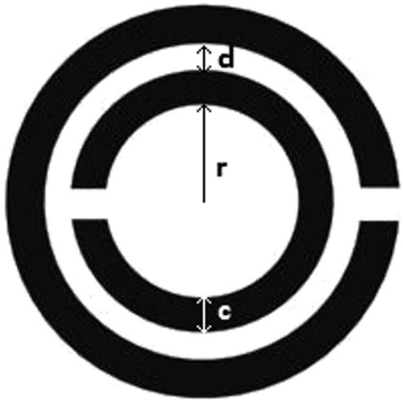

FIG. 1. Schematic representation of the Split Ring Resonator (SRR) with its structural parameters—inner radius (r), ring width (c), and spacing (d).

where the inductance L and capacitance C are dependent upon its structural parameters and permittivity of both the substrate and the surrounding medium.

A. Capacitance of SRR

Quasi-static analysis shows that the capacitance produced between the two rings is due to opposite charges induced on them. It is reasonable to imagine that charges are equally distributed on both upper and lower surfaces of the SRR and hence the fringing electric field distribution may be similar on both sides. The expected field and the charge distribution of the SRR are shown in Fig. 2.

We have experimentally verified the presence of the field and its contribution to the capacitance on both surfaces of the SRR by using a SRR ($r = 2$ mm, $c = 1$ mm, and $d = 0.1$ mm) fabricated on a thin polymer film having no thick substrate.[28] For this, a copper sheet of 20 μm thickness is fixed on an adhesive polymer film of thickness 18 μm, and the SRR structure is fabricated on it using a chemical etching method. A piece of the same polymer film is fixed on the other side of the SRR for the structure to be symmetric. Accordingly, the small capacitive contribution due to the thin polymer films on both sides of the SRR will be the same. In fact, the effect of the polymer films on both sides can be neglected due to their small thickness. The resonant frequency of this structure is measured to be 4.14 GHz. A dielectric sheet of permittivity 2.45 and thickness 1.52 mm is fixed on one side of the SRR, which shifts the resonant frequency to 3.75 GHz. The corresponding shift in the resonant frequency is 0.39 GHz. Another piece of the same material is then placed on the top surface of the SRR, and the resonant frequency is further shifted by 0.36 GHz to 3.39 GHz. Fig. 3 shows these shifts in resonant frequency. Almost equal shifts in resonant frequency verify the presence of equal field distribution on both the upper and lower surfaces of the SRR. Hence, the effective capacitance of the SRR must include the contribution from both semicircular halves of upper and lower sides of the SRR. We have considered this contribution to evaluate the effective capacitance of the structure and to calculate the dielectric constant of various materials in relation to the resonant frequency of the SRR. Since the charge distribution on the two semicircular halves of the SRR rings is opposite, the equivalent representation of capacitance of SRR is shown in Fig. 4. C_1 is the capacitance of the upper semicircular half of the resonator and C_2 is that of the lower semicircular half.

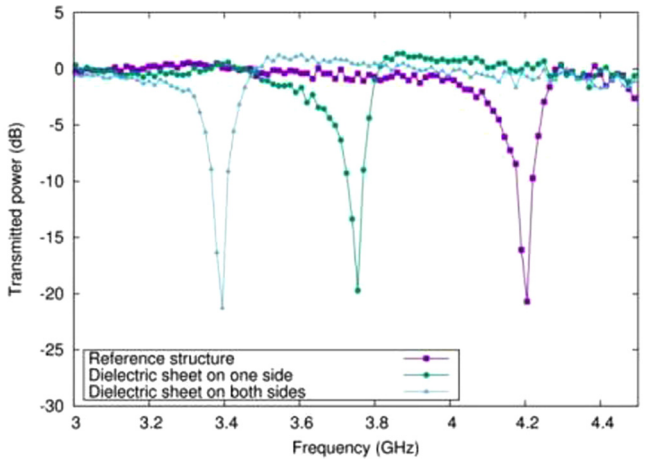

FIG. 3. Transmission curves showing nearly equal shifts in resonant frequency when similar dielectrics are placed on both surfaces of the SRR.

Starting from the basic equation of a parallel plate capacitor, we derive the total capacitance of the SRR by considering the contributions from both faces. If the region above the SRR is filled with a material of dielectric constant ϵ_{r1} up to a thickness sufficient to accommodate the entire fringing fields between the two rings of the structure, the equation of capacitance C_1 is obtained[5] by including the effect of ϵ_{r1} and d as

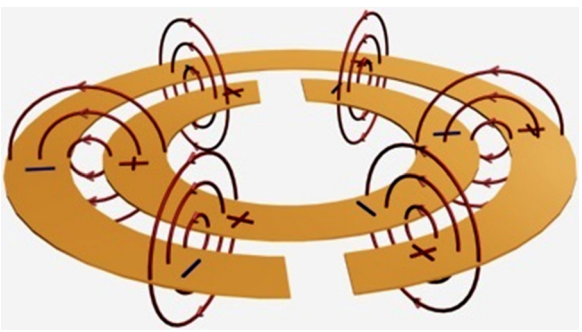

FIG. 2. The representation of the electric field and charge distribution on both surfaces of the SRR.

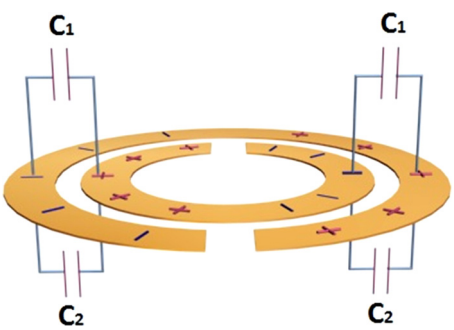

FIG. 4. Equivalent representation of capacitance C_1 and C_2 on upper and lower surfaces of SRR.

$$C_1 = \frac{\epsilon_0 \epsilon_{r1}}{\pi} ln\left(\frac{2c+d}{d}\right)\pi r_{av}, \tag{2}$$

where r_{av} is the average radius of the two rings. Considering a similar behaviour for capacitance C_2 in terms of another dielectric of permittivity ϵ_{r2}, we write the total capacitance C_{tot} of the SRR as

$$C_{tot} = \frac{\epsilon_0}{\pi} ln\left(\frac{2c+d}{d}\right)\pi r_{av}\left(\frac{\epsilon_{r1}+\epsilon_{r2}}{2}\right). \tag{3}$$

Here, we have taken C_{tot} as the parallel combination of the total capacitance of the upper and the lower side of the SRR. Accordingly, we can write

$$C_{tot} \propto (\epsilon_{r1}+\epsilon_{r2})/2. \tag{4}$$

Since the inductance L of the SRR is independent of the permittivity, the resonant frequency can be correlated to ϵ_{r1} and ϵ_{r2} through C_{tot}.

B. Permittivity calculation—real part

From the above relations, we can evaluate the permittivity of the unknown sample if the SRR is fabricated on a substrate with a known or unknown dielectric constant.

1. Calculation in terms of known substrate permittivity ϵ_{r1}

If we consider a SRR with a substrate of known dielectric constant ϵ_{r1} on one side and air on the other side, the resonant frequency f_1 can be represented by using Eqs. (1) and (4) as

$$f_1 \propto \frac{1}{\sqrt{\frac{\epsilon_{r1}+1}{2}}}. \tag{5}$$

When a dielectric sample of the unknown dielectric constant ϵ_{r2} is placed on the surface of the resonator, the resonant frequency changes to

$$f_2 \propto \frac{1}{\sqrt{\frac{\epsilon_{r1}+\epsilon_{r2}}{2}}}. \tag{6}$$

By taking the ratio of Eqs. (5) and (6), we obtain the expression for the unknown dielectric constant of the sample as

$$\epsilon_{r2} = \left[\left(\frac{f_1}{f_2}\right)^2(\epsilon_{r1}+1)\right] - \epsilon_{r1}. \tag{7}$$

A plot between ϵ_{r2} and f_2 for different substrates of relative permittivity ϵ_{r1} is plotted in Fig. 5 using Eq. (7).

2. If the permittivity of the substrate is unknown

When the substrate material itself is used as the sample of the dielectric constant ϵ_{r1}, the resonant frequency will be

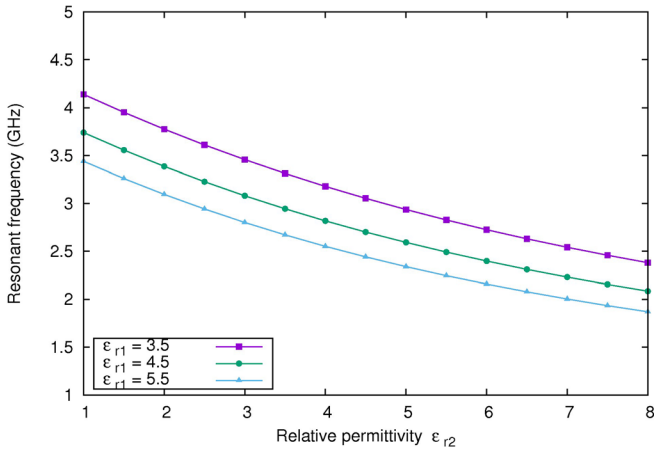

FIG. 5. Plot showing the variation of the resonant frequency f_2 with dielectric constant of the sample ϵ_{r2} for different substrate values ϵ_{r1}.

$$f_2 \propto \frac{1}{\sqrt{\epsilon_{r1}}}. \tag{8}$$

By taking the ratio of Eqs. (5) and (8), we can find the relative permittivity of the substrate material as

$$\epsilon_{r1} = \left[2\left(\frac{f_2}{f_1}\right)^2 - 1\right]^{-1}. \tag{9}$$

Hence, the measurement of the permittivity of a material becomes a simple numerical calculation from the two resonant frequency values f_1 and f_2 even without knowing the permittivity of the substrate, on which the resonator is etched.

C. Permittivity calculation—imaginary part

The imaginary part of the complex permittivity is evaluated in terms of the loss factor tanδ. For a resonant cavity, the expression for tanδ is given by

$$\frac{1}{Q_L} - \frac{1}{Q_0} = \tan\delta, \tag{10}$$

where Q_0 and Q_L are the quality factors of the cavity without and with the sample. In the case of the SRR resonator, the quality factor is measured from the absorption curve by considering the +3 dB bandwidth from transmission minimum.[29–31] Here Q_0 is replaced with Q_{L0}, which will be the quality factor of the SRR resonator when a lossless sample ($\tan\delta = 0$) of the material is assumed to be placed over the experimental probe. Q_L is the quality factor of SRR when the actual sample ($\tan\delta \neq 0$) is placed over it. The corresponding equation is given as

$$\frac{1}{Q_L} - \frac{1}{Q_{L0}} = \tan\delta, \tag{11}$$

Q_{L0}, which will be always greater than Q_L, can be evaluated from the energy equations as follows:

$$Q_{L0} = \frac{(\epsilon_{r1}+\epsilon_{r2})Q_{p0}}{(\epsilon_{r1}+1)}, \tag{12}$$

where Q_{p0} is the quality factor of the SRR test probe.

TABLE I. Structural parameters and resonant frequencies of SRRs used for the measurement.

Test probe	Inner radius -r (mm)	Width of the ring -c (mm)	Spacing -d (mm)	Resonant frequency -f_1 (GHz)
SRR-1	2.0	0.75	0.5	3.456
SRR-2	1.625	0.68	0.4	4.317
SRR-3	1.3	0.65	0.4	4.926
SRR-4	1.0	0.6	0.4	5.697

III. FABRICATION AND EXPERIMENTAL SETUP

SRRs of four different dimensions are constructed using a photochemical etching method on a glass epoxy board. The structural parameters of SRRs and their respective resonant frequencies are given in Table I. The unknown dielectric samples should have at least one flat surface of area greater than or equal to the area of the SRR structure so that they come in close contact with the full area of the resonator surface without any air gap. The thickness of the dielectric is so chosen that the electric field of the resonating structure is completely inside the sample. It has been experimentally verified that a thickness greater than or equal to $c + d/2$ will be sufficient for maximum inclusion of the field which is also evident from the theoretical view point. This thickness condition should be satisfied for the substrate also.

For the measurement of the resonant frequency, a single SRR is placed between transmitting and receiving probes, which are connected to a Vector Network Analyser (VNA). Fig. 6 shows the schematic arrangement and photograph of a test probe. The sample whose dielectric constant is to be measured is placed on the top of the test probe as shown in Fig. 7.

Initially, the resonant frequency of the SRR-1 with known substrate permittivity ϵ_{r1} when no test sample placed over it is measured (f_1). Measurements are then repeated using dielectric samples and their corresponding resonant frequencies are noted (f_2). Using Eq. (7), their dielectric constants (ϵ_{r2}) are calculated. In case, if the substrate permittivity is not known, before using test samples, a piece of the substrate material of the SRR itself is used as the sample and the corresponding resonant frequency is noted as f_2 and using Eq. (9) ϵ_{r1} of the substrate is found out. Measurements are repeated using other three SRRs for all the samples.

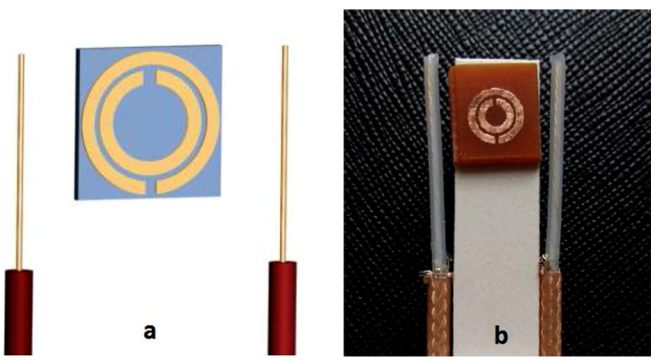

FIG. 6. Schematic arrangement (a) and photograph (b) of the SRR test probe.

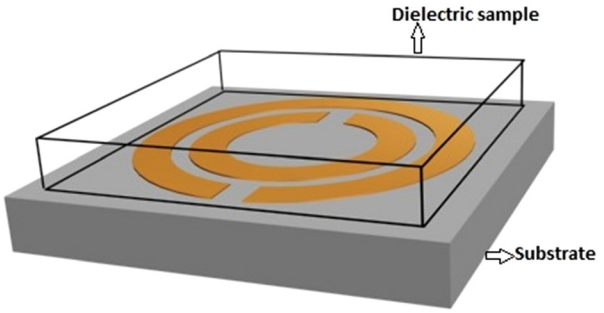

FIG. 7. Schematic representation of the SRR test probe and the dielectric sample.

From Eq. (11), the loss factor tanδ of all the samples is calculated. Q_{p0} and Q_L are obtained from their corresponding transmission curves, and Q_{L0} is calculated for each sample using Eq. (12).

For a comparative study, the dielectric constants of all the samples are measured using a cavity perturbation technique. Thin specimens of the samples are inserted in a waveguide cavity connected to the VNA. Using the dimensions of both the cavity and the sample, by observing the shift in the resonant frequency, the dielectric constants are calculated using equations of the cavity perturbation method.[32] The corresponding loss factors are measured from the calculated quality factors using Eq. (10).

IV. RESULTS AND DISCUSSION

Five samples that are selected for study are glass, perspex, plastic, and two different glass epoxy sheets out of which one is a piece of the substrate itself. Fig. 8 shows the transmission curves of all the five samples along with that of the test probe (SRR-2) as reference. It is observed that the resonant frequencies are shifted towards lower frequencies in relation to their permittivity values. This shift is in agreement with the results predicted by various numerical and simulation methods.[21,24,33,34] The resonant frequency of the

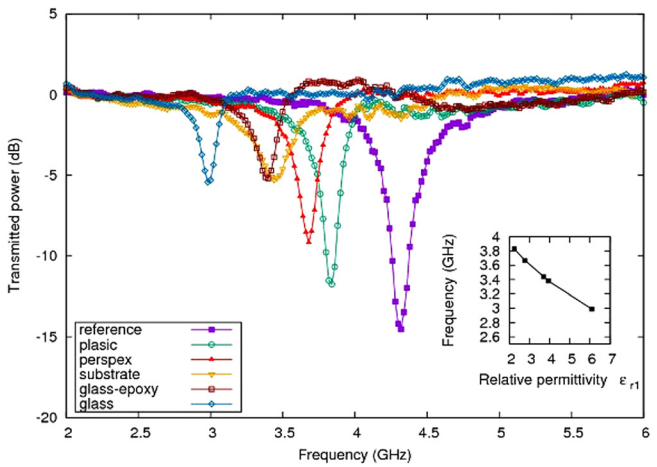

FIG. 8. Transmission spectra showing resonant frequencies of SRR for different samples. Inset shows the calculated relative permittivity values for corresponding resonant frequencies.

SRR-2 is observed to be 4.317 GHz. Out of the five samples used, the minimum frequency shift is for plastic and maximum is for glass. The corresponding resonant frequencies observed are 3.835 GHz and 2.992 GHz, respectively. The resonant frequencies of other three samples are in between these two values as depicted in Fig. 8. The real part of the relative permittivity values is calculated using Eq. (7), and it is plotted as the inset graph. The loss factors of all the five samples are evaluated using Eq. (11). As expected, the plastic sample is almost lossless (≈0.003), while the glass epoxy and the substrates of the SRR show relatively high loss factors (≈0.03 to 0.04). The other two samples of perspex and glass have $\tan\delta$ values around 0.01. The accuracy of these measured values also depends upon the frequency interval between measurement points (sampling interval). By reducing the sampling interval, we can more precisely locate the resonance dip, which helps in a more accurate determination of the results. The sampling interval of the order of few MHz will not change the accuracy of the results considerably. The maximum change in the $\tan\delta$ values due to the possible slight change in locating the resonant dip obtained in our measurements is—glass epoxy $= \pm 0.00000024$, substrate $= \pm 0.000001$, glass $= \pm 0.000000053$, plastic $= \pm 0.00045$, and perspex $= \pm 0.00037$. Table II gives the resonant frequencies in GHz along with the calculated values of the dielectric constant and $\tan\delta$ for all the samples evaluated using the four SRR test probes. The thickness of the sample and the dielectric constant along with the loss factors measured using cavity perturbation method are also included in this table. The values obtained by our method using SRR test probes are closely in agreement with that obtained from the cavity method. Thus by simply placing the sample over the SRR test probe or by placing the test probe over the sample (cases of bulk samples), we are able to precisely measure the dielectric constant and the loss factor.

Advantages of this SRR resonant method over other resonant dielectric measurement techniques are the ease in sample preparation and the simplicity in experimental setup, which include only a SRR test probe connected to a VNA. The permittivity equations used for the calculations are also very simple. Since our SRR probe is not coupled directly with a guided wave, the theoretical formulation is straight forward and simple when compared with transmission line based SRR systems. The only condition for precise analysis is that the sample thickness should be such that the field of the resonator is completely inside the sample. This technique is extremely preferable for samples of bulk size.

It is observed that the measurement using SRR does not fully agree with the standard values as the dielectric constant increases beyond a certain limit. The relations for capacitance and permittivity given earlier are valid when the quasi-static nature is maintained for the magnetic field component. The equations for the capacitance are developed by assuming that the field over the SRR is almost constant. But when a dielectric sample of high permittivity is placed over the probe, the wavelength of the field across SRR within the sample reduces by a factor of $1/\sqrt{\epsilon_r}$. In such situations, it deviates from the quasi-static approximation and the linear relationship between the capacitance and the permittivity does not hold perfectly. Then the equation for the equivalent capacitance may not be expressed in the form as given in Section II. In such conditions, we can reduce the dimensions of the SRR, which may enhance the accuracy of measurements.

When we look into the performance efficiency of our method in comparison with some of the standard methods,[35–38] the following points may be noted. In comparison with the waveguide method, the free space method, and the cavity perturbation method, the selection of size and shape of the experimental sample offers more flexibility here. All the advantages of the transmission line method such as rapid and easy measurement and the ability to use at various temperature levels are equally possible here along with the added feature of the provision to move the test probe towards a sample if the situation demands so. Apart from the above mentioned advantages, this is a non-destructive testing technique, which may find use in the case of costly and rare samples. Since we are employing a movable test probe, the method can be easily extended to the permittivity characterization of liquids by using it as a submersible probe. The air gap error usually happening in the coaxial method and in the planar transmission line method can be effectively minimized by proper mounting of the sample over the SRR. The presence of the air gap changes the effective permittivity, and hence a small reduction in the resonant frequency shift is expected. This may result in a slightly lower value for the real and imaginary parts of the permittivity. Hence, for accurate results in our method, care should be taken to maintain the constant environmental conditions so as not to disturb the field distribution around the test probe during the measurements. We can also expect slight errors in experimental

TABLE II. Values of complex permittivity obtained by using four different SRR test probes in comparison with the cavity perturbation method.

		Test probes													
		SRR-1			SRR-2			SRR-3			SRR-4			Cavity perturbation	
Sample	Thickness (mm)	f_2	ϵ_r	$\tan\delta$	f_2	ϵ_r	$\tan\delta$	f_2	ϵ_r	$\tan\delta$	f_2	ϵ_r	$\tan\delta$	ϵ_r	$\tan\delta$
Plastic	2.85	3.090	2.124	0.0039	3.835	2.259	0.0031	4.379	2.21	0.0035	5.020	2.310	0.0034	2.302	0.0036
Perspex	2.12	3.006	2.471	0.0151	3.679	2.776	0.0131	4.277	2.522	0.0122	4.911	2.574	0.0151	2.459	0.0143
Glass epoxy	3.1	2.741	3.695	0.0332	3.386	3.944	0.0361	3.860	3.861	0.0370	4.483	3.804	0.0420	3.767	0.0351
Substrate	2.71	2.763	3.571	0.0380	3.445	3.714	0.0371	3.930	3.662	0.0411	4.560	3.554	0.0462	3.583	0.0380
Glass	2.66	2.402	5.891	0.0121	2.992	6.099	0.0094	3.360	6.357	0.0105	3.907	6.128	0.0108	6.073	0.0115

values due to surface imperfection of the sample and SRR fabrication errors.

V. CONCLUSION

In this paper, we have introduced a simple and effective method for the measurement of permittivity of low dielectric constant samples at microwave frequencies using a metamaterial Split Ring Resonator. Equations for the dielectric constant and the loss tangent, in terms of the resonant frequency and bandwidth of the transmission curve, are derived from the basic equivalent circuit parameters of SRR. Measurements are carried out for five dielectric samples using four SRR test probes. Results are found to be in excellent agreement with that measured using cavity perturbation techniques. The ease of sample preparation, the simplicity in the experimental setup, and the direct calculation of permittivity make this method a very efficient one for the precise determination of the complex permittivity. By reducing the frequency interval between neighbouring measurement points, the accuracy of the result can be further increased. In addition to this, our proposed model may find potential uses in a wide variety of sensors and scanning applications such as nondestructive surface imperfection study and bio-medical imaging.

[1]E. Nyfors and P. Vainikainen, *Industrial Microwave Sensors*, Artech House Microwave Library (Artech House, 1989).

[2]L. F. Chen, C. Ong, C. Neo, V. V. Varadan, and V. K. Varadan, *Microwave Electronics: Measurement and Materials Characterization* (John Wiley & Sons, 2004).

[3]K. Saeed, M. F. Shafique, M. B. Byrne, and I. C. Hunter, *Planar Microwave Sensors for Complex Permittivity Characterization of Materials and Their Applications*, edited by Md. Zahurul Haq (InTech, 2012), p. 319.

[4]J. Sheen, "Study of microwave dielectric properties measurements by various resonance techniques," Measurement **37**, 123–130 (2005).

[5]J. B. Pendry, A. J. Holden, D. Robbins, and W. Stewart, "Magnetism from conductors and enhanced nonlinear phenomena," IEEE Trans. Microwave Theory Tech. **47**, 2075–2084 (1999).

[6]D. R. Smith and N. Kroll, "Negative refractive index in left-handed materials," Phys. Rev. Lett. **85**, 2933 (2000).

[7]D. R. Smith, W. J. Padilla, D. Vier, S. C. Nemat-Nasser, and S. Schultz, "Composite medium with simultaneously negative permeability and permittivity," Phys. Rev. Lett. **84**, 4184 (2000).

[8]T. Koschny, P. Markoš, D. Smith, and C. Soukoulis, "Resonant and antiresonant frequency dependence of the effective parameters of metamaterials," Phys. Rev. E **68**, 065602 (2003).

[9]D. Smith, S. Schultz, P. Markoš, and C. Soukoulis, "Determination of effective permittivity and permeability of metamaterials from reflection and transmission coefficients," Phys. Rev. B **65**, 195104 (2002).

[10]S. P. Chakyar, J. Andrews, and V. P. Joseph, "Temperature dependence of relative permittivity: A measurement technique using split ring resonators," Int. J. Mech., Aerosp., Ind., Mechatronic Manuf. Eng. **10**, 1030–1033 (2016).

[11]M. Labidi, J. B. Tahar, and F. Choubani, "Meta-materials applications in thin-film sensing and sensing liquids properties," Opt. Express **19**, A733–A739 (2011).

[12]W. Withayachumnankul, K. Jaruwongrungsee, A. Tuantranont, C. Fumeaux, and D. Abbott, "Metamaterial-based microfluidic sensor for dielectric characterization," Sens. Actuators, A **189**, 233–237 (2013).

[13]M. S. Boybay and O. M. Ramahi, "Non-destructive thickness measurement using quasi-static resonators," IEEE Microwave Compon. Lett. **23**, 217–219 (2013).

[14]C.-S. Lee and C.-L. Yang, "Thickness and permittivity measurement in multi-layered dielectric structures using complementary split-ring resonators," IEEE Sens. J. **14**, 695–700 (2014).

[15]R. Melik, E. Unal, N. K. Perkgoz, C. Puttlitz, and H. V. Demir, "Metamaterial based telemetric strain sensing in different materials," Opt. Express **18**, 5000–5007 (2010).

[16]R. Melik, E. Unal, N. K. Perkgoz, C. Puttlitz, and H. V. Demir, "Flexible metamaterials for wireless strain sensing," Appl. Phys. Lett. **95**, 181105 (2009).

[17]H. Karim, D. Delfin, M. A. I. Shuvo, L. A. Chavez, C. R. Garcia, J. H. Barton, S. M. Gaytan, M. A. Cadena, R. C. Rumpf, R. B. Wicker *et al.*, "Concept and model of a metamaterial-based passive wireless temperature sensor for harsh environment applications," IEEE Sens. J. **15**, 1445–1452 (2015).

[18]Z. Jakšić, O. Jakšić, Z. Djurić, and C. Kment, "A consideration of the use of metamaterials for sensing applications: Field fluctuations and ultimate performance," J. Opt. A: Pure Appl. Opt. **9**, S377 (2007).

[19]G. Puccetti, U. Reggiani, and L. Sandrolini, "Experimental analysis of wireless power transmission with spiral resonators," Energies **6**, 5887–5896 (2013).

[20]F. Bilotti, A. Toscano, L. Vegni, K. Aydin, K. B. Alici, and E. Ozbay, "Equivalent-circuit models for the design of metamaterials based on artificial magnetic inclusions," IEEE Trans. Microwave Theory Tech. **55**, 2865–2873 (2007).

[21]E. Ekmekci and G. Turhan-Sayan, "Comparative investigation of resonance characteristics and electrical size of the double-sided SRR, BC-SRR and conventional srr type metamaterials for varying substrate parameters," Prog. Electromagn. Res. B **12**, 35–62 (2009).

[22]T. Weiland, R. Schuhmann, R. Greegor, C. Parazzoli, A. Vetter, D. Smith, D. Vier, and S. Schultz, "Ab initio numerical simulation of left-handed metamaterials: Comparison of calculations and experiments," J. Appl. Phys. **90**, 5419–5424 (2001).

[23]S.-Y. Chiam, R. Singh, W. Zhang, and A. A. Bettiol, "Controlling metamaterial resonances via dielectric and aspect ratio effects," Appl. Phys. Lett. **97**, 191906 (2010).

[24]Z. Sheng and V. V. Varadan, "Tuning the effective properties of metamaterials by changing the substrate properties," J. Appl. Phys. **101**, 014909 (2007).

[25]J. Naqui, J. Coromina, F. Martín, A. K. Horestani, and C. Fumeaux, "Comparative analysis of split ring resonators (srr), electric-lc (elc) resonators, and s-shaped split ring resonators (s-srr): Potential application to rotation sensors," in *Proceedings of 2014 Mediterranean Microwave Symposium (MMS2014)* (IEEE, 2014), pp. 1–5.

[26]M. Boybay and O. M. Ramahi, "Material characterization using complementary split-ring resonators," IEEE Trans. Instrum. Meas. **61**, 3039–3046 (2012).

[27]G. Galindo-Romera, F. J. Herraiz-Martínez, M. Gil, J. J. Martínez-Martínez, and D. Segovia-Vargas, "Submersible printed split-ring resonator-based sensor for thin-film detection and permittivity characterization," IEEE Sens. J. **16**, 3587–3596 (2016).

[28]P. M. Ragi, K. S. Umadevi, P. Nees, J. Jose, M. V. Keerthy, and V. P. Joseph, "Flexible split-ring resonator metamaterial structure at microwave frequencies," Microwave Opt. Tech. Lett. **54**, 1415–1416 (2012).

[29]H.-J. Lee, H.-S. Lee, K.-H. Yoo, and J.-G. Yook, "DNA sensing using split-ring resonator alone at microwave regime," J. Appl. Phys. **108**, 014908 (2010).

[30]I. M. Rusni, A. Ismail, A. R. H. Alhawari, M. N. Hamidon, and N. A. Yusof, "An aligned-gap and centered-gap rectangular multiple split ring resonator for dielectric sensing applications," Sensors **14**, 13134–13148 (2014).

[31]A. Fulford, "Conductor and dielectric property extraction using microstrip tee resonators," Ph.D. thesis (Auburn University, 2005).

[32]K. T. Mathew, "Perturbation theory," in *Encyclopedia of RF and Microwave Engineering* (John Wiley & Sons, Inc., 2005).

[33]E. Ekmekci and G. Turhan-Sayan, "Sensitivity of the resonance characteristics of SRR and DSRR (double-sided SRR) type metamaterials to the changes in substrate parameters and the usefulness of DSRR structure for reduced electrical size," in *PIERS Proceedings* (2008), pp. 598–602.

[34]R. Marqués, F. Mesa, J. Martel, and F. Medina, "Comparative analysis of edge-and broadside-coupled split ring resonators for metamaterial design-theory and experiments," IEEE Trans. Antennas Propag. **51**, 2572–2581 (2003).

[35]J. Baker-Jarvis, M. D. Janezic, and D. C. DeGroot, "High-frequency dielectric measurements," IEEE Instrum. Meas. Mag. **13**, 24–31 (2010).

[36]A. P. Gregory and R. N. Clarke, "A review of rf and microwave techniques for dielectric measurements on polar liquids," IEEE Trans. Dielectr. Electr. Insul. **13**, 727–743 (2006).

[37]S. Nelson *et al.*, "Dielectric properties of agricultural products and some applications," Res. Agric. Eng. **54**, 104–112 (2008).

[38]P. Bernard and J. Gautray, "Measurement of dielectric constant using a microstrip ring resonator," IEEE Trans. Microwave Theory Tech. **39**, 592–595 (1991).